Reservoir water-level drawdowns accelerate and amplify methane emission

Authors:

J.A. Harrison[1,†] , B.R. Deemer[1], M.K. Birchfield[1], and M.T. O'Malley[1,2]

This Supplementary Information section is 15 pages long, and contains supplemental methods, 9 supplemental figures, two supplemental tables, and associated references.

Supplemental information

Supplemental Methods

Echosounder Transects

In each study reservoir we performed hydroacoustic transects using a Biosonics 120 Hz, split-beam transducer as in Ostrovsky et al. (2008)[1] . In each case, the transducer was deployed attached to the hull of a 16' Boston Whaler traveling <5 kmph during periods both before drawdown and during drawdown. Visual Acquisition 6.0 software was used to visualize and analyze hydroacoustic data qualitatively for bubble densities. Average target strengths of bubbles were calculated and related to bubble sizes, but these data were not used to calculate per-area fluxes in this analysis. Rather bubble densities from hydracoustic surveys were compared qualitatively with trap-based measurements, and showed general correspondence over space and time. Two representative sets of surveys from Lacamas Lake and J. C. Boyle reservoir are included below (Figs S5 and S6). In Lacamas Lake, surveys conducted prior to spill showed fewer hydroacoustic reflectances than surveys conducted during spill (compare S8a and b). Spatial patterns in hydroacoustic reflectances in Lacamas were also consistent with trap-estimated CH_4 ebullition fluxes, with the highest bubble densities toward the inlet end of the lake. Similarly, a hydroacoustic survey conducted in J.C. Boyle Reservoir early in a drawdown event showed much lower bubble densities than a survey conducted well into a drawdown event, and the region of highest bubble density (the portion of J.C. Boyle Reservoir near its dam) was also the region of highest estimated CH_4 ebullition based on trap sampling (Figure S9).

Figure and Table Legends

Figure S1. Locations of reservoirs included in this study; inset at upper left shows location of expanded map of Oregon and Washington within the US.

Figure S2. Maps of study reservoirs indicating placement of funnel traps used in this study in 2013 (X or * symbols) and in 2014 and 2015 in Lacamas Lake (points). Profile sampling sites are also indicated (* symbols); note different scales for each map (Source for all base maps in this figure: Map data © 2016 Google).

Figure S3. One of the bubble traps used in this study. Collection funnel is located at the base of the trap and the housing for a logging differential pressure transducer is located at the top. Meter stick at left is included for scale.

Figure S4. Methane concentration (%) in field standards (y-axis) as a function of time of deployment in field control chambers (days).

Figure S5. Time series showing A) change in the water surface elevation anomaly in Lacamas Lake (secondary Y-axis and black lines), and B) annual cumulative bubbled volume of gas in traps (ml accumulated over the year-to-date) located at four sites in Lacamas Lake in 2011 and 2012, six sites in 2013, and 13 sites in 2014-2015; lines represent individual bubble traps, and

points represent sampling events where traps were emptied and gas concentrations were measured. Annual reservoir drawdown events are indicated by shaded gray bars.

Figure S6. Average pre-drawdown and during-drawdown CH_4 concentrations (mg CH_4 L^{-1}) in the epilimnion (top panel) and hypolimnion (bottom panel) of study reservoirs.

Figure S7. Panel A) excess mass of CH_4 (total mass of CH_4 minus equilibrium CH_4) in the hyplimnion of Lacamas Lake (kg CH_4) over a 5 year period (left-hand y axis and black points) and the water level anomaly for Lacamas (right-hand y-axis and black lines). Panel B) Excess mass of CH_4 in hypolimnion of Cle Elum reservoir. Panel C) Excess mass of CH_4 in hypolimnion of Kachess reservoir. In all panels drawdown events are highlighted with shaded bars.

Figure S8. Hydroacoustic reflectances >-65 dB prior to a water level drawdown event (A) and during a water level drawdown event (B) in Lacamas Lake during September 2013. Panels A and B represent cross-sections of the reservoir, with the area at the left of the plots falling closest to the reservoir outlet and the area at the right of the plot falling mid-reservoir. Pathway of transect is shown in panel C on right.

Figure S9. Hydroacoustic reflectances >-65 dB (represented by gray points) early in a water level drawdown event (A) and toward the end of a water level drawdown event (B) in J.C. Boyle reservoir during August 2013. Panels A and B represent cross-sections of the reservoir, with the area at the left of the plot being closest to the reservoir outlet and the area at the right of the plot falling mid-reservoir. Pathway of transect is shown in panel C on right as are the locations of the 4 ebullition traps that were deployed on the reservoir during the transect period (small circles).

Table S1. Diffusive, ebullitive, and total CH_4 fluxes (mg CH_4 m^{-2} d^{-1}) from reservoirs in this study compared with reservoir CH_4 emissions from other studies. Total reservoir fluxes from other reservoirs represent datasets where both diffusive and ebullitive CH_4 fluxes were measured. Median CH_4 fluxes from other reservoirs are presented with ranges in parentheses. For fluxes estimated in this study, n values represent number of profiles averaged to estimate diffusive flux estimates, number of CH_4 traps used for ebullition fluxes, and number of systems included in the database of other reservoirs with CH_4 emission data. Uncertainties are reported as ± 1 standard error. Bold text indicates CH_4 fluxes in the top 10% of any reported fluxes.

Table S2. Average rates of bubble emission from study reservoirs (ml m^{-2} d^{-1}) with ranges of observed rates over period of measurement (Table 2) in parentheses.

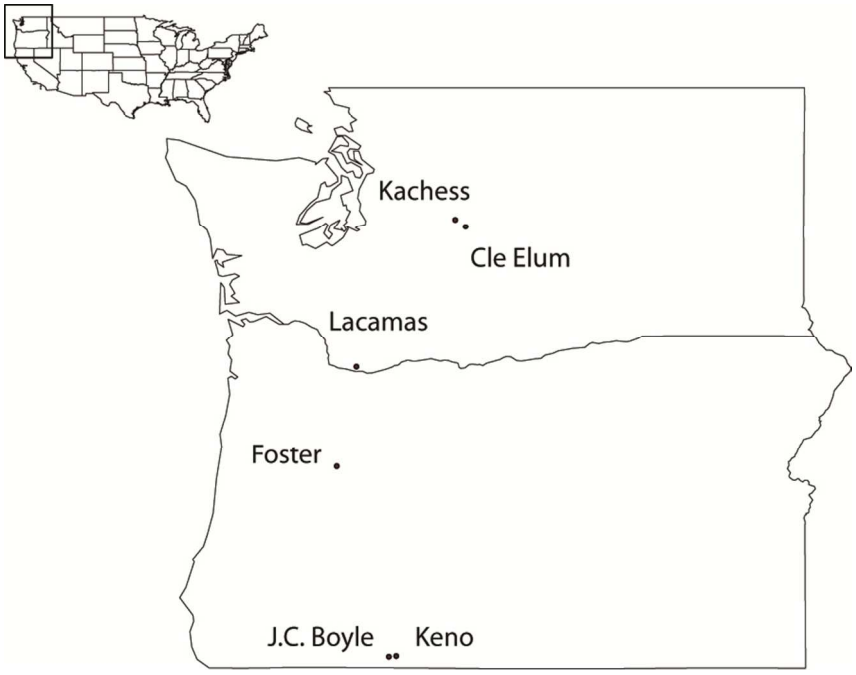

Figure S1. Locations of reservoirs included in this study; inset at upper left shows location of expanded map of Oregon and Washington within the US.

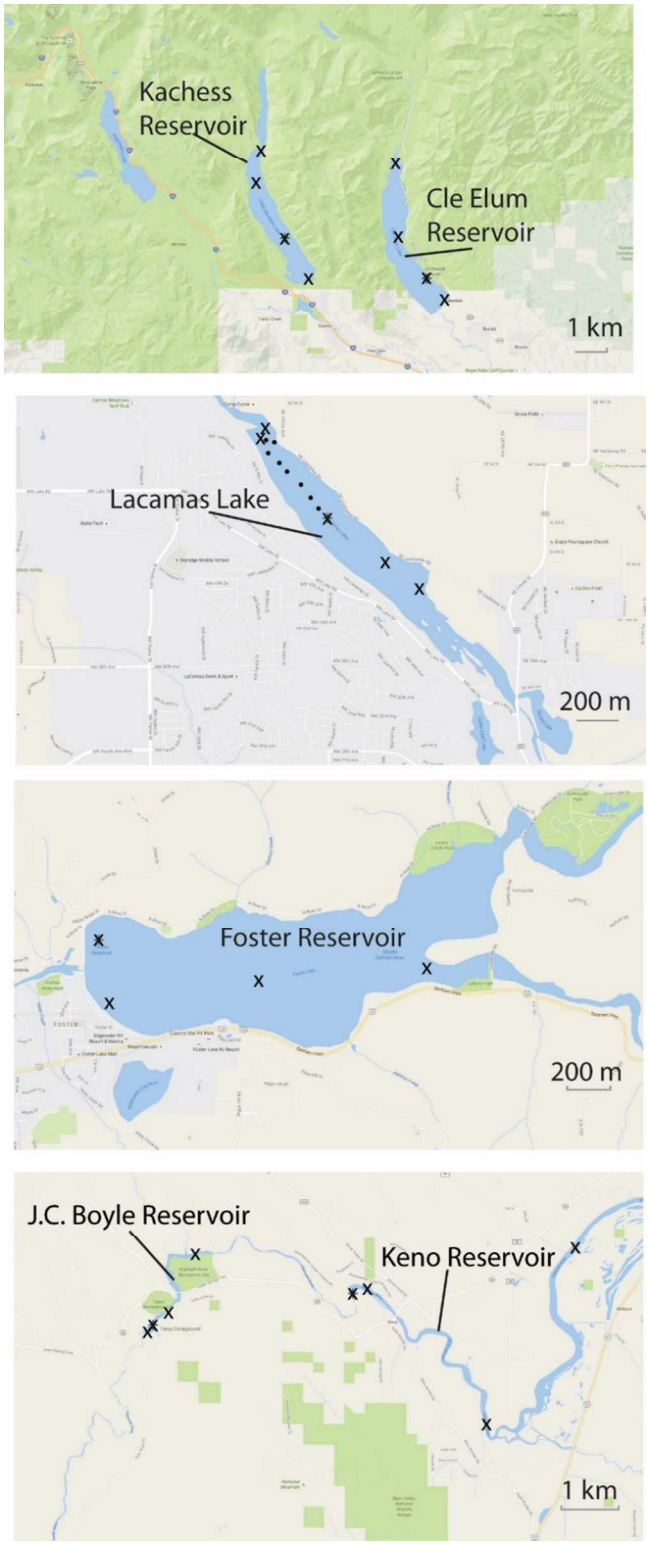

Figure S2. Maps of study reservoirs indicating placement of funnel traps used in this study in 2013 (X or * symbols) and in 2014 and 2015 in Lacamas Lake (points). Profile sampling sites, the deepest points in each reservoir, are also indicated (* symbols); note different scales for each map (Source for all base maps in this figure: Map data © 2016 Google).

Figure S3. One of the bubble traps used in this study. Collection funnel is located at the base of the trap and the housing for a logging differential pressure transducer is located at the top. Meter stick at left is included for scale.

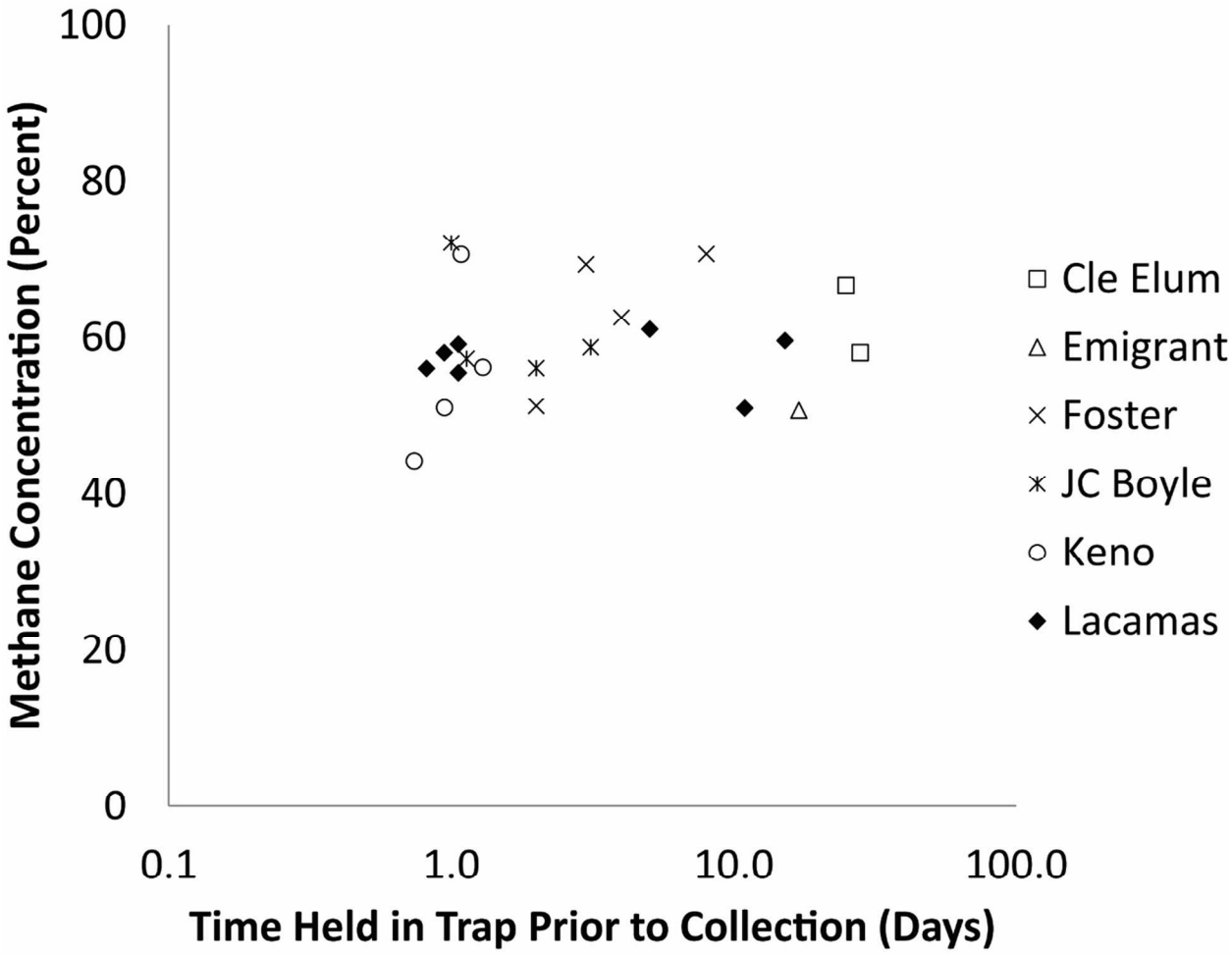

Figure S4. Methane concentration (%) in field standards (y-axis) as a function of time of deployment in field control chambers (days). One control trap was deployed in each reservoir and all sampling events included sampling of a control trap.

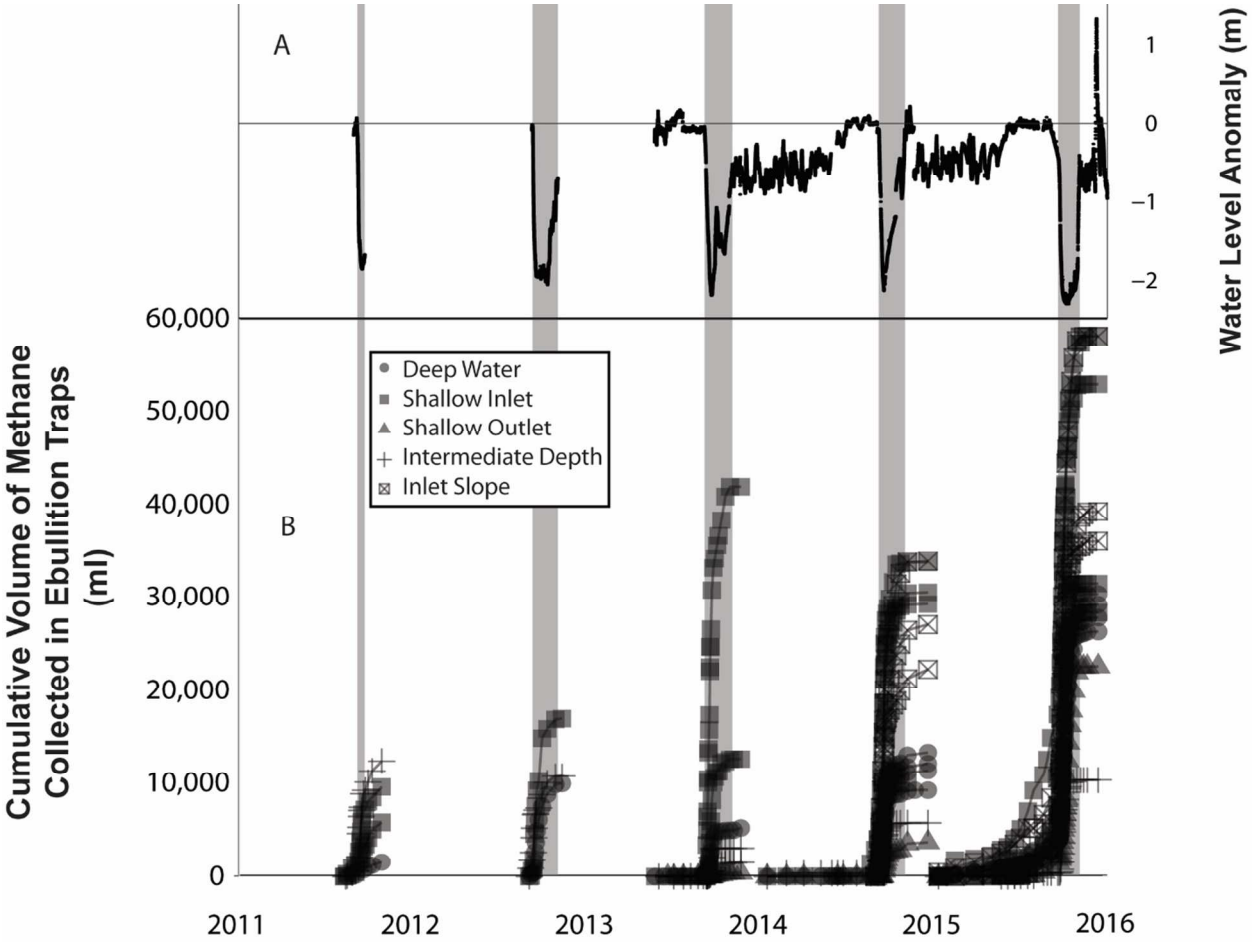

Figure S5. Time series showing A) change in the water surface elevation anomaly in Lacamas Lake (secondary Y-axis and black lines), and B) annual cumulative bubbled volume of gas in traps (ml accumulated over the year-to-date) located at four sites in Lacamas Lake in 2011 and 2012, six sites in 2013, and 13 sites in 2014-2015; lines represent individual bubble traps, and points represent sampling events where traps were emptied and gas concentrations were measured. Annual reservoir drawdown events are indicated by shaded gray bars.

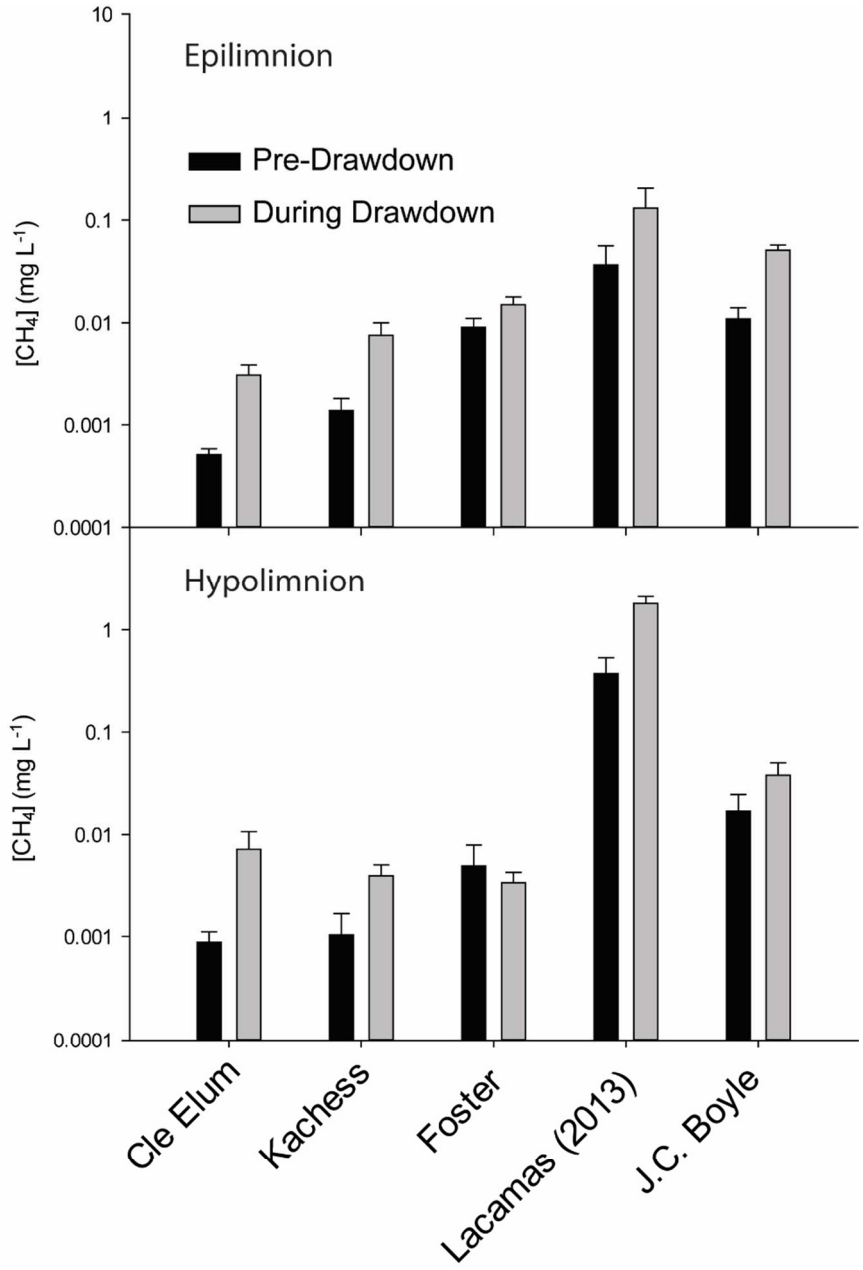

Figure S6. Average pre-drawdown and during-drawdown CH_4 concentrations (mg CH_4 L^{-1}) in the epilimnion (top panel) and hypolimnion (bottom panel) of study reservoirs.

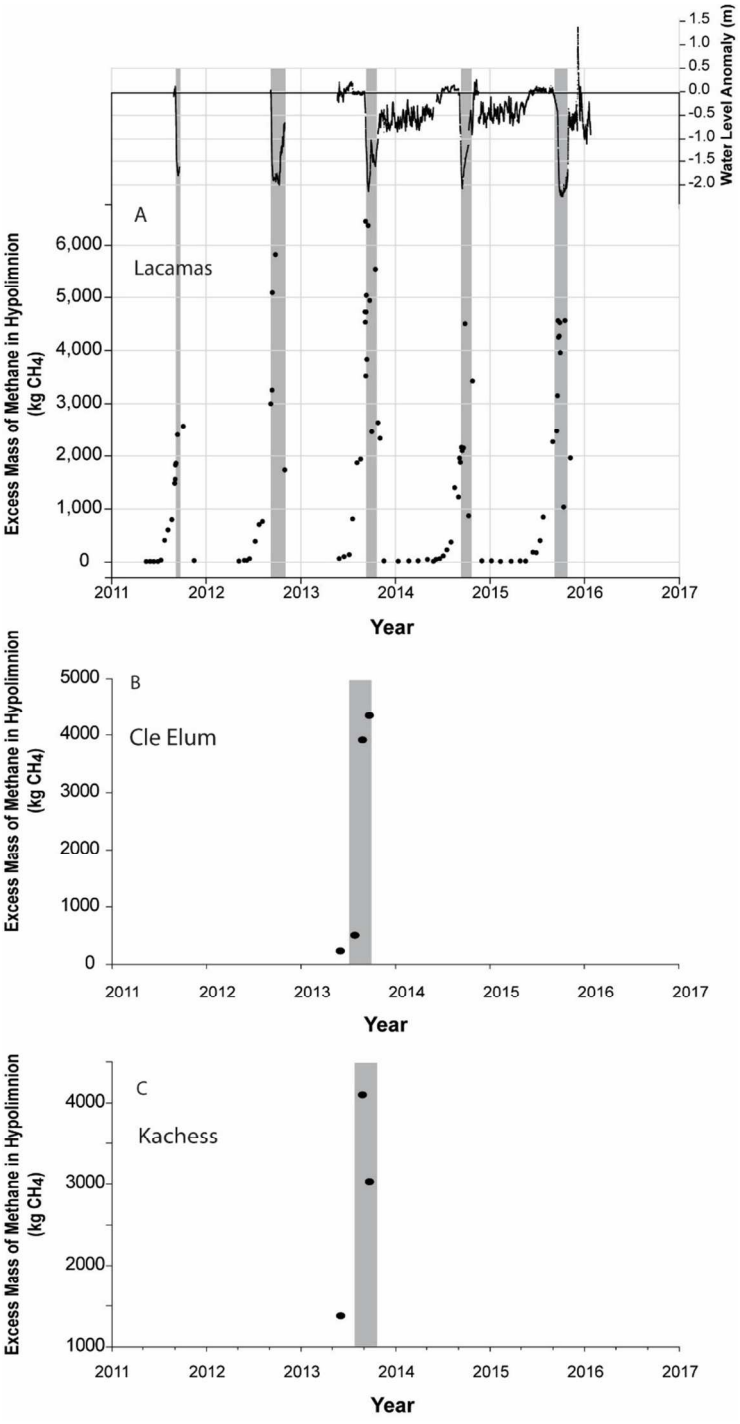

Figure S7. Panel A) excess mass of CH_4 (total mass of CH_4 minus equilibrium CH_4) in the hyplimnion of Lacamas Lake (kg CH_4) over a 5 year period (left-hand y axis and black points) and the water level anomaly for Lacamas (right-hand y-axis and black lines). Panel B) Excess mass of CH_4 in hypolimnion of Cle Elum reservoir. Panel C) Excess mass of CH_4 in hypolimnion of Kachess reservoir. In all panels drawdown events are highlighted with shaded bars.

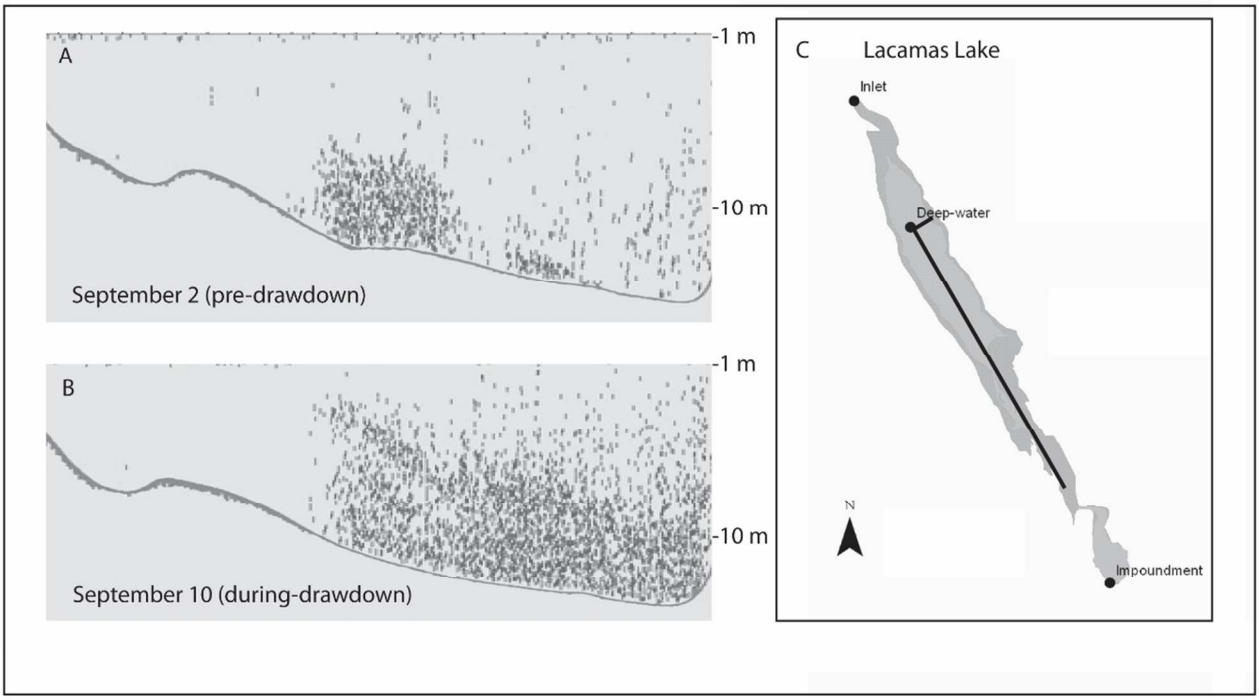

Figure S8. Hydroacoustic reflectances >-65 dB prior to a water level drawdown event (A) and during a water level drawdown event (B) in Lacamas Lake during September 2013. Panels A and B represent cross-sections of the reservoir, with the area at the left of the plots falling closest to the reservoir outlet and the area at the right of the plot falling mid-reservoir. Pathway of transect is shown in panel C on right.

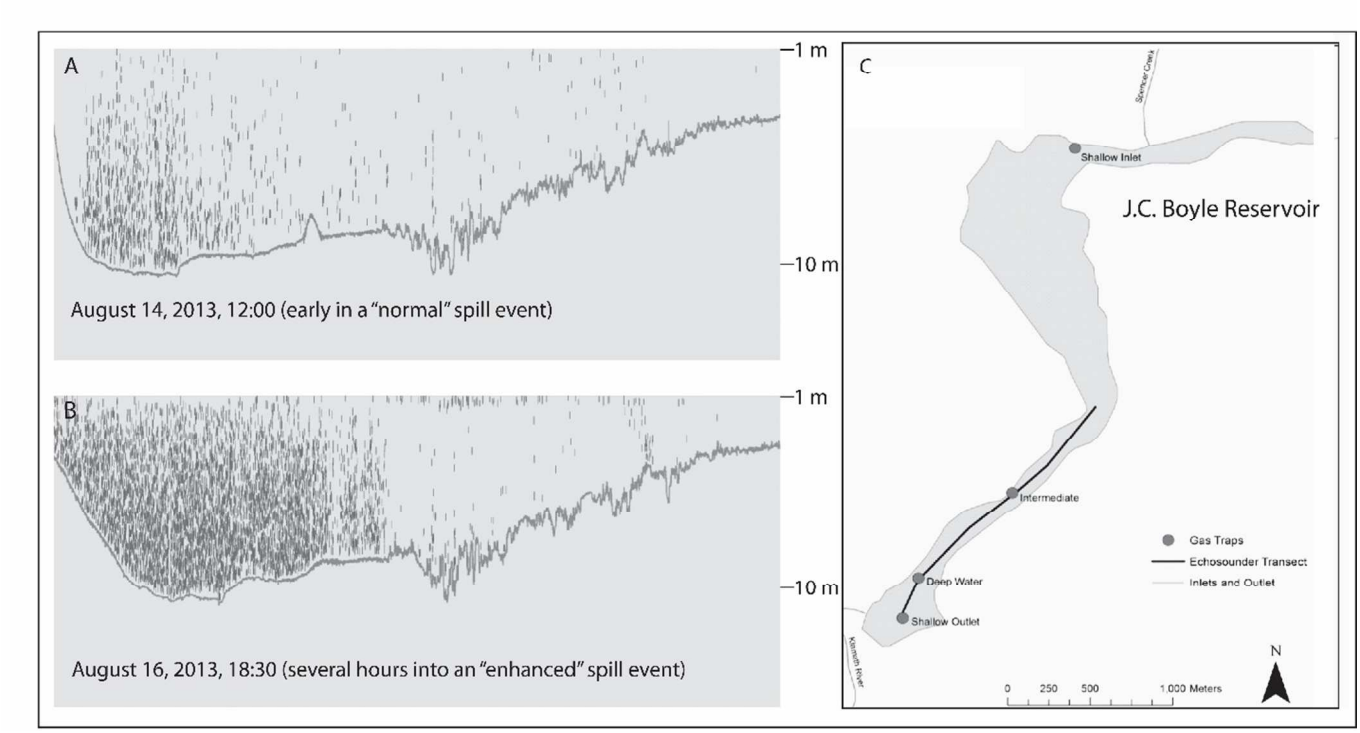

Figure S9. Hydroacoustic reflectances >-65 dB (represented by gray points) early in a water level drawdown event (A) and toward the end of a water level drawdown event (B) in J.C. Boyle reservoir during August 2013. Panels A and B represent cross-sections of the reservoir, with the area at the left of the plot being closest to the reservoir outlet and the area at the right of the plot falling mid-reservoir. Pathway of transect is shown in panel C on right as are the locations of the 4 ebullition traps that were deployed on the reservoir during the transect period (small circles).

Table S1. Diffusive, ebullitive, and total CH_4 fluxes (mg CH_4 m^{-2} d^{-1}) from reservoirs in this study compared with reservoir CH_4 emissions from other studies. Total reservoir fluxes from other reservoirs represent datasets where both diffusive and ebullitive CH_4 fluxes were measured. Median CH_4 fluxes from other reservoirs are presented with ranges in parentheses. For fluxes estimated in this study, n values represent number of profiles averaged to estimate diffusive flux estimates, number of CH_4 traps used for ebullition fluxes, and number of systems included in the database of other reservoirs with CH_4 emission data. Uncertainties are reported as ± 1 standard error. Bold text indicates CH_4 fluxes in the top 10% of any reported fluxes.

Reservoir and Drawdown Conditions	**Diffusive Flux**	**Ebullition Flux**	**Total**
Lacamas 2013 Pre-Drawdown	8.44 ± 1.07	0.03 ± 0.02	8.47 ± 1.09
Lacamas 2013 During Drawdown (Sep 8 - 24)	12.42 ± 1.97	212.29 ± 173.10	224.71 ± 175.07
Cle Elum 2013 Pre-Drawdown (Jun 4 – Jul 29)	0.21 ± 0.03	0.00 ± 0.00	0.21 ± 0.03
Cle Elum 2013 During Drawdown (Jul 29 – Sep 7)	1.49 ± 0.36	1.57 ± 1.54	3.06 ± 1.90
Kachess 2013 Pre-Drawdown (Jun 6 – July 31)	0.75 ± 0.26	0.04 ± 0.04	0.79 ± 0.30
Kachess 2013 During Drawdown (Aug 1 – Oct 8)	5.32 ± 2.11	1.03 ± 1.91	6.35 ± 4.02
Foster 2013 Pre-Drawdown (Aug 6 – Oct 2)	2.1 ± 0.18	17.63 ± 10.76	19.73 ± 10.94
Foster 2013 During Drawdown (Oct 2 – Oct 16)	7.60 ± 0.41	169.66 ± 121.91	177.26 ± 122.32
J.C. Boyle 2013 Pre-Drawdown (00:00 - 08:00 each day)	8.22 ± 2.04	192.59 ± 106.67	200.81 ± 108.71
J.C. Boyle 2013 During Drawdown (10:00 – 20:00 each day)	38.03 ± 0.69	**719.73 ± 398.19**	**757.76 ± 398.88**
Keno 2013	13.93 ± 2.79	**310.65 ± 85.40**	**324.58 ± 88.19**
Other Reservoirs [2]	56.83 (0–5247.30; n=140)	101.41 (0-733.10; n=50)	160.47 (0.05-2292.72; n=75)

Table S2. Average rates of bubble emission from study reservoirs (ml m^{-2} d^{-1}) with ranges of observed rates over period of measurement (Table 2) in parentheses.

Reservoir	**Bubble Release Rate (ml m^{-2} d^{-1})**
Lacamas	89.0 (0 - 22,158.9)
Cle Elum	2.74 (0 - 46.3)
Kachess	10.2 (0 – 43.9)
Foster	177.9 (0 – 1,847.7)
J.C. Boyle	985.6 (0 – 33,898.7)
Keno	340.4 (0 – 1273.2)

References

1. Ostrovsky, I.; McGinnis, D. F.; Lapidus, L.; Eckert, W., Quantifying gas ebullition with echosounder: the role of methane transport by bubbles in a medium-sized lake. *Limnol Oceanogr-Meth* **2008,** *6*, 105-118.
2. Deemer, B. R.; Harrison, J. A.; Li, S.; Beaulieu, J. J.; DelSontro, T.; Barros, N.; J.F.Bezerra-Neto; Powers, S. M.; Santos, M. A. d.; Vonk, J. A. Greenhouse Gas Emissions from Reservoir Water Surfaces: A New Global Synthesis. *BioScience* **2016**, *66 (11): 949-964*.